

Adaptive Sensing for Instantaneous Gas Release Parameter Estimation

Vassilios N. Christopoulos and Stergios Roumeliotis

Dept. of Computer Science & Engineering, University of Minnesota, Minneapolis, MN 55454

Email: {vchristo|stergios}@cs.umn.edu

Abstract—This paper presents a new approach for estimating in real-time the parameters of the advection-diffusion equation that describes the propagation of an instantaneously released gas. A mobile robot equipped with an appropriate sensing device collects measurements in order to estimate the parameters of this equation. The selection of the set of locations where chemical concentration measurements should be recorded, is performed in real-time with the objective of maximizing the accuracy of the parameter estimates and reducing the time to convergence of this estimation problem. Simulation results are presented that validate the described approach, which has significantly lower computational requirements compared to alternative motion strategies based on exhaustive global search.

I. INTRODUCTION

In the post-Cold War era and after the terrorist attacks on September 11, 2001, there is a growing concern that future terrorist activities may involve the use of chemical or biological weapons, such as in the attack with the nerve gas Sarin in the Tokyo subway in 1995 [1]. In addition, there is a number of unintentional chemical agent explosions, such as an accidental release from a chemical refining or storage area, as the Union Carbide release in Bhopal, India [2]. In each situation, a quantity of hazardous material is released in the atmosphere creating dangerous or lethal conditions for people. Furthermore, the chemical agent particles may be spread by the wind and affect areas outside the immediate proximity of the initial release. Dealing with these scenarios requires that specially trained individuals are able to accurately and rapidly predict the consequences of the release, estimate its spread, and determine emergency response actions such as evacuating populated areas and/or attempting to contain the agent by spraying appropriate chemical absorbents.

Successful prediction is conditioned on the availability of accurate information regarding the gas release. Propagation models based on the advection-diffusion equation (Eq. (2)) require precise knowledge of the release time t_0 and location (x_0, y_0, z_0) , the amount of gas release (mass Q), and the dispersion coefficients \mathbf{K} for this chemical agent in a given environment. In many cases, sufficient prior knowledge is unavailable or potentially inaccurate. Thus, these parameters should be estimated by collecting gas concentration measurements from the region of explosion. This in turn requires that individuals in protective equipment enter the hazardous area and obtain samples.

In an ideal situation, this sampling task could be achieved

by mobile robots. This would require that these robots are equipped with sensors for measuring the concentration of the chemical agent, registering the locations and times where measurements were recorded, and processing this information to compute accurate estimates for the parameters of the advection-diffusion equation. Robots with these capabilities will reduce the risk to the human response teams and potentially lower the financial cost of such operations since no life support equipment is necessary for a robotic emergency response team.

However, due to the time-critical nature of the problem, simply requiring that the robots perform a random or exhaustive search of the affected area may not be sufficient for quickly establishing accurate estimates of the parameters of the release. A robot must be able to determine a trajectory, described as a set of feasible next locations, that it must follow in order to acquire the most informative measurements, i.e., the measurements that will improve the accuracy of the estimates for the parameters of the advection-diffusion equation. This paper presents a method for accomplishing precisely this task in the case of a single robot that can localize outdoors by means of GPS. This initial approach operates in a reasonably simplified environment, relatively flat and obstacle free, in order to establish the feasibility of the proposed method.

II. RELATED WORK

A. Source Localization methods

A number of methods inspired by the behavior of species for identification of airborne or waterborne agents, have been proposed for the solution of the odor localization problem. *Chemotaxis* and *Anemotaxis* are the most common techniques used in nature. Chemotaxis relies on the local gradient of the chemical agent concentration while Anemotaxis-based approaches require that the agent moves in the upwind direction. Even though both these methods are well-accepted for Chemical Plume Tracing (CPT), they suffer from two significant drawbacks. Chemotaxis is not feasible in an environment with a medium or high Reynolds number, where it could lead to regions with high concentration that are not the source (e.g., the corner of a room) [3]. Anemotaxis, on the other hand, should not be applied in an environment without strong ventilation [4].

1) *Concentration Gradient-based*: The Adapted Moth Strategy is employed for odor localization in an unventilated environment [5]. A mobile robot or, a team of robots,

equipped with a gas sensor performs a random search until it identifies concentration of the chemical agent. Thereafter, the robot starts a zigzag motion by turning approximately 65° to the side of the highest concentration. When the robot completes six zigzag turns, it executes a circular motion with a radius of 50cm. If the sensors record an increased value of the gas concentration, the motion pattern is restarted. A biased random walk approach to CPT is presented in [6]. A mobile robot records concentration measurements and localizes multiple sources by employing two modes. In the first one, named “run”, the robot navigates towards the source by computing the local gradient. In the second mode, named “tumble”, the robot randomly reorients itself in a new direction, which will be the direction of the next run. After performing a run, if the sensors record a positive gradient, it decreases the tumbling frequency and increases the run length. A negative gradient triggers a tumble without affecting its frequency.

2) *Flow Direction-based*: A number of methods have been inspired by the general perception that diffusion is a slower mass-transfer mechanism compared to wind. Based on this observation, a robotic system, equipped with anemometric devices and gas sensors, was designed by Ishida et al [7]. This work presents two approaches to source localization. In the first one, called “step-by-step”, the robot moves at an angle in-between the direction against the wind and that towards the gas sensor with the highest response. In the second approach, called “zigzag”, the vehicle moves obliquely upwind across the plume. Once it reaches the boundary of the plume, it changes direction and heads towards the boundary on the opposite side. An extension of this work to environments where there is no uniform wind direction is presented in [8]. As long as the gas sensors receive reliable measurements, the robot computes and follows the local gradient. When it reaches a region of low concentration, it turns and moves upwind.

In [9], a mobile robot equipped with a chemical sensor, a bumper sensor, and a wind vane, moves in an indoor environment in order to detect a chemical leak. Initially, the robot calculates the location of the plume centroid by collecting measurements of the gas concentration across the plume. Subsequently, it moves towards the center and against the wind until it detects the source. The Spiral Surge Algorithm [10] is one of the most popular CPT algorithms in the field of Swarm Intelligence. A mobile robot follows a spiral trajectory collecting data of the gas concentration. Once a plume is detected, the robot moves in the upwind direction for a specific time interval. If the plume is detected again, the robot continues the upwind trajectory, otherwise it starts a new spiral trajectory in order to re-encounter the plume.

A behavior-based approach to CPT for an Autonomous Underwater Vehicle (AUV) is presented in [11]. Initially, the AUV searches for chemical traces by moving obliquely to the current. Once a plume is detected, the robot moves against the direction of the flow. If the chemical distribution becomes intermittent, e.g., due to turbulent fluid flow, the

robot continuous to move mostly up-flow, but at a varying angle. Finally, if no measurements are available, over a large time interval, it switches to a reacquisition behavior and follows a clover leaf shaped trajectory.

3) *Fluid Dynamics-based*: A CPT approach based on principles of fluid dynamics is presented in [3], [4]. This method, referred to as *Fluxotaxis*, relies on the computation of the one-dimensional Gradient of Divergence of Mass Flux (GDMF) in order to lead a team of autonomous agents to the location of the chemical emitter.

Methods previously used for predicting meteorological phenomena and pollution tracking, such as the Ensemble Kalman filter [12], have also been applied to the odor localization problem. The Process Query System (PQS) is appropriate for filtering large numbers of data originating from a network of sensors [13]. In this work, the source location determination is formulated as a two-dimensional inverse problem based on the diffusion equation.

At this point, we should note that the aforementioned methods can be used for source localization and *not* for estimating the parameters of the advection-diffusion equation that describes the *propagation* or *spread* of the chemical.

B. Spread Estimation methods

A number of methods have been developed for predicting the spread of a chemical agent after a gas explosion. Most of these are based on the computation of the advection-diffusion equation parameters. This equation describes the propagation of an instantaneously released gas as a function time [14]. A method for estimating six of the parameters that appear in the advection-diffusion equation is proposed in [15]. In this work, measurements of the gas concentration are collected and the parameter values are estimated offline. This is known as inverse modelling and has been formulated as a nonlinear least-squares estimation problem. Extensions to [15] are presented in [16], [17] for the case of a continuously released chemical agent.

Finally, a technique for modelling the distribution of the chemical agent concentration in an unventilated indoor environment is presented in [18]. A mobile robot is used for producing a grid-map description of the area. An estimated value of the gas concentration is assigned to each cell of the grid.

III. ADVECTION - DIFFUSION MODEL

The approach presented in this paper uses the advection-diffusion model developed in [15]. In this model, a standard Cartesian coordinate system is used with the X -axis coinciding with the mean wind direction. An instantaneous release of Q kg of gas occurs at time t_0 at location (x_0, y_0, z_0) . This is then spread by the wind with mean velocity $\mathbf{U} = [u, 0, 0]^T$. The concentration, C , of the released agent at an arbitrary location (x, y, z) and time t is described by the following equation:

$$\frac{\partial C}{\partial t} = -\nabla \mathbf{q} \quad (1)$$

Vector \mathbf{q} represents the total mass of all particles of the released substance which move through a location within a given time interval.

A. Solving the Advection - Diffusion equation

Solving Eq. (1) requires determining both the initial and boundary conditions. Assuming that the release of the contaminant is instantaneous, the initial conditions can be modelled by a Dirac delta function at (x_0, y_0, z_0) . Boundary conditions result from the following two observations: (i) the concentration is zero at infinity in all spatial directions, and (ii) it is assumed that the contaminant is not absorbed by the ground.

In order to simplify the derivation, certain factors, such as the structure of the landscape and variations in humidity, are not taken into consideration. Furthermore, to allow for a closed-form solution, the velocity of the wind, u , as well as the eddy diffusivities, K_x , K_y and K_z are assumed to be constant. Under these assumptions, the solution of Eq. (1) is:

$$C(x, y, z, t) = \frac{Q}{8\pi^{\frac{3}{2}} (K_x K_y K_z)^{\frac{1}{2}} (\Delta t)^{\frac{3}{2}}} \times e^{-\frac{(\Delta x - u\Delta t)^2}{4K_x\Delta t} - \frac{\Delta y^2}{4K_y\Delta t}} \times \left(e^{-\frac{\Delta z^2}{4K_z\Delta t}} + e^{-\frac{\Delta z'^2}{4K_z\Delta t}} \right) \quad (2)$$

where $\Delta x = x - x_0$, $\Delta y = y - y_0$, $\Delta z = z - z_0$, $\Delta z' = z + z_0$ and $\Delta t = t - t_0$. For the problem at hand, a mobile robot is used to collect concentration measurements. Unless special custom-designed robots are used, it is clear that the measurements can only take place very close to the ground. We model this situation by assuming that all measurements are recorded at $z = 0$, and the release occurs at ground level, i.e., $z_0 = 0$. Thus, Eq. (2) can be modified as follows:

$$C(x, y, 0, t) = \frac{Q}{4\pi^{\frac{3}{2}} (K_x K_y K_z)^{\frac{1}{2}} (\Delta t)^{\frac{3}{2}}} \times e^{-\frac{(\Delta x - u\Delta t)^2}{4K_x\Delta t} - \frac{\Delta y^2}{4K_y\Delta t}} \quad (3)$$

This expression resembles a Gaussian function, with time varying standard deviations along both the X and Y axes. A visualization of the solution is depicted in Fig. 1.

B. Problem Formulation

We now focus on the inverse problem of determining the parameters of the instantaneous gas release from measurements of the gas concentration. We seek to estimate the location (x_0, y_0) and time t_0 of the explosion, the gas release mass Q , and the eddy diffusivities along the X and Y axes, assumed to be equal, $K_x = K_y$ ¹. The wind velocity u is provided by an anemometer and is treated as a known constant.

We formulate a least-squares estimation problem for determining the parameter vector $\boldsymbol{\theta} = [Q \ K_x \ x_0 \ y_0 \ t_0]^T$, using measurements Z_k of the concentration $C_k =$

¹ K_z can be found by using models, such as those described in [19].

$C(x_k, y_k, 0, t_k; \boldsymbol{\theta})$ of the chemical agent corrupted by zero-mean white Gaussian noise $n(t_k)$:

$$Z_k = C_k + n(t_k) \quad (4)$$

where $\sigma_n^2 = E[n(t_k)^2]$ is the variance of this noise.

From Eq. (3), the following expression for the natural logarithm of the gas concentration is derived:

$$h_k(\boldsymbol{\theta}) = \ln C_k = \ln \left(\frac{Q}{4\pi^{\frac{3}{2}} (K_x K_y K_z)^{\frac{1}{2}}} \right) - \frac{3}{2} \ln(\Delta t) - \left(\frac{\Delta x^2}{4K_x} + \frac{\Delta y^2}{4K_x} \right) \frac{1}{\Delta t} - \frac{u^2 \Delta t}{4K_x} + \frac{2u\Delta x}{4K_x} \quad (5)$$

Note that this formula contains no exponential terms, which greatly simplifies the following derivations. Eq. (5) relates the logarithm of the concentration to the parameter vector $\boldsymbol{\theta}$, defined above. The natural logarithm of each measurement of the concentration, \bar{Z}_k , is given by:

$$\bar{Z}_k = \ln(C_k + n(t_k)) \simeq \ln C_k + \bar{n}(t_k) \quad (6)$$

where $\bar{n}(t_k)$ is a noise process corrupting the logarithm of the concentration.

At this point, a comment regarding the distribution of the samples of the noise process $\bar{n}(t_k)$ is necessary. The basic assumption is that the measurement noise is a white, zero-mean, Gaussian process. Thus, it is expected that the noise affecting the logarithm of the concentration is not Gaussian. However, by plotting the empirically determined, through Monte Carlo simulations, histogram of the samples of this noise process, shown in Fig. 2, we can observe that the spread of $\bar{n}(t_k)$ can be well approximated by a Gaussian probability density function (pdf). Linearization of Eq. (6) yields

$$\bar{n}(t_k) \simeq \frac{1}{C_k} n(t_k) \quad (7)$$

Thus the variance $\sigma_{\bar{n}}^2$ (scalar) of \bar{n} is given by:

$$\sigma_{\bar{n}}^2 = E[\bar{n}^2(t_k)] = \frac{1}{C_k^2} E[n^2(t_k)] = \frac{\sigma_n^2}{C_k^2} = \frac{1}{\alpha^2} \quad (8)$$

where α^2 is the signal to noise ratio (SNR), assumed to be constant.

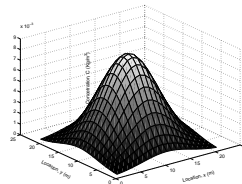


Fig. 1. 2D gas distribution.

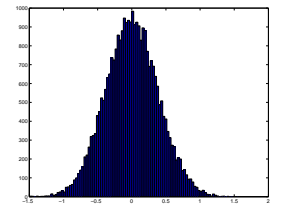


Fig. 2. Log noise histogram.

The cost function we seek to minimize is

$$f(\boldsymbol{\theta}) = (\bar{\mathbf{Z}} - \mathbf{h}(\boldsymbol{\theta}))^T \mathbf{R}^{-1} (\bar{\mathbf{Z}} - \mathbf{h}(\boldsymbol{\theta})) \quad (9)$$

where $\bar{\mathbf{Z}} = [\bar{Z}_1 \dots \bar{Z}_N]^T$ is the vector of all (logarithmic) measurements collected by the robot, $\mathbf{h}(\boldsymbol{\theta}) = [h_1(\boldsymbol{\theta}) \dots h_N(\boldsymbol{\theta})]^T$ is the vector of the corresponding expected measurements and $\mathbf{R} = \sigma_n^2 \mathbf{I}_{N \times N}$ is the measurement noise matrix. It is clear that f is a nonlinear function of the elements of $\boldsymbol{\theta}$ and cannot be solved in closed form for $\boldsymbol{\theta}$. Therefore, we resort to linearization of this formula by employing the Taylor series expansion $\mathbf{h}(\boldsymbol{\theta}) \simeq \mathbf{h}(\hat{\boldsymbol{\theta}}) + \mathbf{H}(\boldsymbol{\theta} - \hat{\boldsymbol{\theta}})$ where $\mathbf{H} = \mathbf{H}(\hat{\boldsymbol{\theta}}) = \begin{bmatrix} \mathbf{H}_1^T & \dots & \mathbf{H}_N^T \end{bmatrix}^T$ is the $N \times 5$ Jacobian matrix of $\mathbf{h}(\boldsymbol{\theta})$. Since there are five parameters in the estimated vector $\boldsymbol{\theta}$, a minimum of five (non-degenerate) concentration measurements are required in order for a unique solution to exist.

C. Levenberg - Marquardt Optimization for estimating $\boldsymbol{\theta}$

In our implementation, the Levenberg-Marquardt method (L-M) has been employed for the iterative minimization of the cost function in Eq. (9). L-M is a combination of the Gauss-Newton and the Steepest Descent methods. It employs function evaluations and gradient information while estimates of the Hessian matrix are computed as the sum of the outer product of the gradients. The behavior of the L-M method is determined by a positive coefficient μ_p . For small values of μ_p , L-M approximates the Gauss-Newton method, whereas for large values of μ_p it behaves as a Steepest Descent. The basic advantage of L-M optimization is its robustness to numerical errors. However, since it is a gradient-based method, under poor initialization it may be attracted to local minimum of the cost function.

Given an initial estimate, from the previous time step, $\hat{\boldsymbol{\theta}}_k^0 = \hat{\boldsymbol{\theta}}_k$, a recursive relation for the vector of the estimated parameters $\hat{\boldsymbol{\theta}}_{k+1} = \hat{\boldsymbol{\theta}}_k^{m+1}$, where m is the last L-M iteration, can be obtained by employing the following iterative process for the minimization of the linearized cost function in Eq. (9):

$$\hat{\boldsymbol{\theta}}_k^{p+1} = \hat{\boldsymbol{\theta}}_k^p + \left(\sum_{i=1}^k \mathbf{H}_i^T \mathbf{H}_i + \frac{\mu_p}{\alpha^2} \cdot \mathbf{I}_{k \times k} \right)^{-1} \times \sum_{i=1}^k \mathbf{H}_i^T (Z_i - h_i(\hat{\boldsymbol{\theta}}_k^p)) \quad (10)$$

Note that all quantities related to $\hat{\boldsymbol{\theta}}$, on the right hand side of this equation, are computed using the estimated parameter vector $\hat{\boldsymbol{\theta}}_k^p$ from the p -th iteration.

The covariance matrix of the estimated parameter vector $\hat{\boldsymbol{\theta}}_k$ is given by

$$\mathbf{P}_k = \frac{1}{\alpha^2} \left(\sum_{i=1}^k \mathbf{H}_i^T \mathbf{H}_i \right)^{-1} \quad (11)$$

IV. TRAJECTORY GENERATION

The selection of the sequence of locations, where the measurements will be recorded is based on the minimization of the uncertainty of the estimated parameter vector $\boldsymbol{\theta}$. This is described by the trace of the *expected* covariance matrix $\hat{\mathbf{P}}_{k+1}$, computed in Eq. (11) using the *expected* values

of the matrices $\mathbf{H}_i(x_i, y_i)$ for any candidate location(s) (x_i, y_i) considered by the robot for collecting the next measurement(s). Through a large number of simulations, the trace of the *expected* covariance matrix was determined to be locally concave. We employ the following theorem, adapted from [20], for minimizing the trace of the *expected* covariance matrix.

Theorem 1: Let f be a function defined on the bounded, closed concave set Ω . If f has a minimum over Ω , it is achieved at an extreme point of Ω .

Fig. 3 shows that the current position of the robot (indicated by the dashed line) is near the point that corresponds to the maximum value of the cost function. Therefore, before recording the next measurement, the robot must move as far away as possible from its current location, towards the boundary of the objective function. Based on this observation, we set the velocity of the robot to its maximum value V_{max} and hereafter we concentrate on determining the set of directions of motion $\phi_k, k = 0 \dots N-1$ that minimize the trace of the *expected* covariance matrix, $\hat{\mathbf{P}}_{k+1}$.

The spatiotemporal distribution of the measurements \mathbf{Z} , processed for determining the parameter vector $\boldsymbol{\theta}$, has a significant impact on the accuracy and the convergence properties of this estimation problem. In general, it is necessary to have at least as many measurements as the number of parameters being estimated. For the case of the instantaneous gas release, a minimum of five measurements is required. It is unrealistic to assume that the measurement times and locations can be selected arbitrarily. Thus, a trajectory generation method must be devised that allows for both accurate and timely estimation of the release parameters. Assume that at time t_k , the robot is located at position (x_k, y_k) . The robot should be able to move at its maximum velocity V_{max} for some sampling time interval ΔT . This provides a set of reachable points that form a circle of radius $r = V_{max} \cdot \Delta T$. Thus, the next location for sampling becomes a function of its heading ϕ_k and is provided by the following equations:

$$x_{k+1} = x_k + r \cos(\phi_k) \quad , \quad y_{k+1} = y_k + r \sin(\phi_k) \quad (12)$$

Schematically, the motion of the robot from one position to another is depicted in Fig. 6.

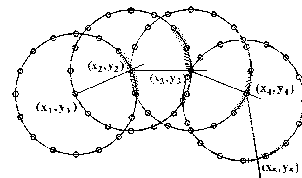


Fig. 6. Robot trajectory for collecting measurements.

A. Globally Optimal Trajectory

Several techniques can be applied to generate the optimal trajectory. Exhaustive search is probably the simplest method and is based on calculating all candidate trajectories and choosing the “best” among them. The optimization criterion, expressed in terms of the set $\mathbf{u} = [\phi_1, \phi_2 \dots \phi_{N-1}]^T$

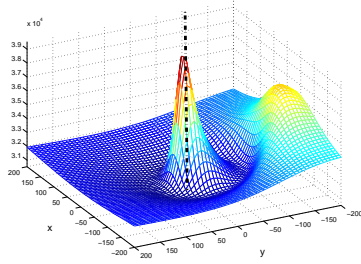


Fig. 3. Cost function (3D plot).

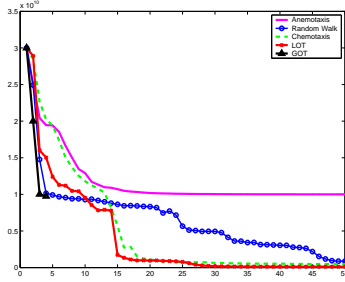


Fig. 4. Trace of the covariance matrix.

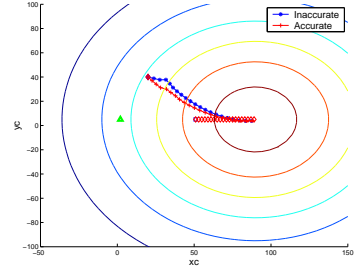


Fig. 5. Robot trajectory with accurate and inaccurate initial estimate for θ (LOT).

of consecutive directions of motion for collecting $N \geq 5$ measurements is:

$$\mathbf{u} = \arg \min_{\{\phi_1 \dots \phi_{N-1}\}} \text{trace} \left(\sum_{i=1}^N \mathbf{H}_i^T(\phi_{i-1}) \mathbf{H}_i(\phi_{i-1}) \right)^{-1}$$

This involves discretizing the reachable set, at each time step (a circle of radius r), into d intervals $\delta\phi_d = 2\pi/d$. If there are $N - 1$ steps along the path, $O(d^{N-1})$ candidate trajectories must be generated and evaluated to determine which of these minimizes the trace of the *expected* covariance matrix $\hat{\mathbf{P}}_N = \frac{1}{\alpha^2} \left(\sum_{i=1}^N \mathbf{H}_i^T \mathbf{H}_i \right)^{-1}$ in the above criterion. For large values of d , this approach is computationally intractable.

While the computations required by an exhaustive search approach may deem it unrealistic, a slightly more restricted version should provide a reasonable approximation. Instead of using a large value for d , a significantly smaller number ℓ is selected. This, initially, generates ℓ large ‘‘slices’’ with an interior angle $\delta\phi_{\ell_1} = 2\pi/\ell$, from which a small and relatively coarse set of trajectories is evaluated. The ‘‘best’’ trajectory is then refined by iteratively reducing the size of $\delta\phi_{\ell}$ around each step in the trajectory, i.e., $\delta\phi_{\ell_{j+1}} = \delta\phi_{\ell_j}/\ell$, $j = 1 \dots n$. This process, depicted in Fig. 6 is repeated n times until $\delta\phi_{\ell_n}$ has reached a desired precision yielding a final total of $O(n \cdot \ell^{N-1})$ trajectories to evaluate. From here on, we will refer to this method as Globally Optimal Trajectory (GOT).

B. Locally Optimal Trajectory

Even the reduced computational requirements of the restricted exhaustive search (GOT), described in Section IV-A, can significantly impair the ability of a mobile robot to react in an emergency situation and collect measurements of a gas concentration in real-time. Hereafter, a new technique is described that makes only one-step ahead prediction for the next position where the robot should move to, in order to register a measurement. This approach, referred hereafter as Locally Optimal Trajectory (LOT), has both a reasonable computational cost and convergence time.

The iterative, one-step optimization process that describes this new motion strategy, is based on the following recursive criterion:

$$u_k = \arg \min_{\phi_k} \text{trace} \left(\mathbf{A}_k + \mathbf{H}_{k+1}^T(\phi_k) \mathbf{H}_{k+1}(\phi_k) \right)^{-1} \quad (13)$$

In this relation, the second term $\mathbf{H}_{k+1}^T(\phi_k) \mathbf{H}_{k+1}(\phi_k)$, is a function of the direction ϕ_k that the robot should follow for collecting its next measurement Z_{k+1} . In $\mathbf{A}_k = \nu_k \mathbf{I}_{5 \times 5} + \sum_{i=1}^k \mathbf{H}_i^T \mathbf{H}_i$, ν_k is a small positive number, constant at each step and is computed based on the set of previous locations x_i , y_i and time instants t_i where the robot recorded measurements Z_i , $i = 1 \dots k$. The term $\nu_k \mathbf{I}_{5 \times 5}$ guarantees invertibility of \mathbf{A}_k while the term $\sum_{i=1}^k \mathbf{H}_i^T \mathbf{H}_i$ corresponds to the information due to the previously collected measurements.

The solution to this optimization problem provides the next best sensing position x_{k+1} , y_{k+1} of the robot for minimizing the uncertainty of the estimate $\hat{\theta}_{k+1}$. Once the robot makes a decision where to go next, it moves there, records a measurement, and employs Eqs. (10) and (11) to update the current state and covariance estimates. The same process is repeated until sufficient number of measurements have been collected to reduce the uncertainty of the estimates for the gas concentration parameters θ below a specified threshold. This method has linear, to the number of measurements N , computational cost and can be implemented on robots with limited processing capabilities.

In [21], we have proven that the cost function in Eq. (13) is equivalent to:

$$u_k = \arg \max_{\phi_k} \left[\frac{\mathbf{H}_{k+1} \mathbf{A}_k^{-2} \mathbf{H}_{k+1}^T}{1 + \mathbf{H}_{k+1} \mathbf{A}_k^{-1} \mathbf{H}_{k+1}^T} \right] \quad (14)$$

This form of the cost function can be approximated by:

$$u_k^* \simeq \arg \max_{\omega} \frac{g_2 \omega^2 + g_1 \omega + g_0}{(s_2 + 2) \omega^2 + s_1 \omega + (s_0 + 1)} \quad (15)$$

where $\omega = \tan\left(\frac{\gamma_k - \phi_k}{2}\right)$ and γ_k is the bearing angle towards the estimated peak of the gas concentration. The scalars g_j and s_j , $j = 0, 1, 2$, are functions of the problem parameters and are given in [21].

V. SIMULATION RESULTS

A. Comparison of the Methods

This section presents a comparison between the LOT method and three of the most popular approaches in the field of chemical agent detection, namely Chemotaxis, Anemotaxis and Random Walk. The results of these methods are also compared to those of the GOT method.

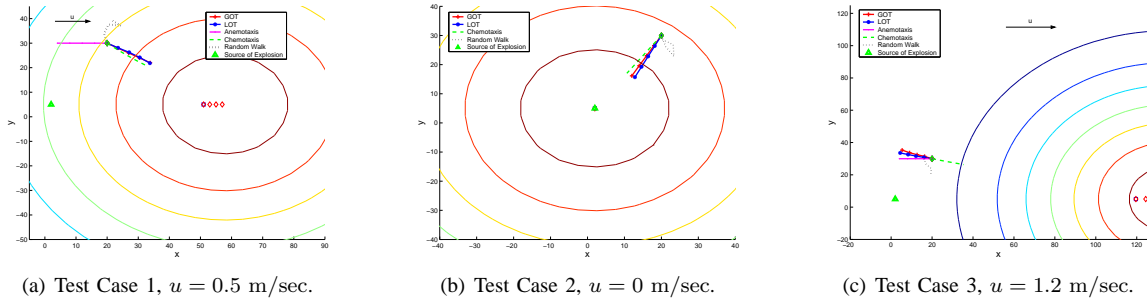


Fig. 7. Comparison of GOT, LOT, Anemotaxis, Chemotaxis and Random Walk.

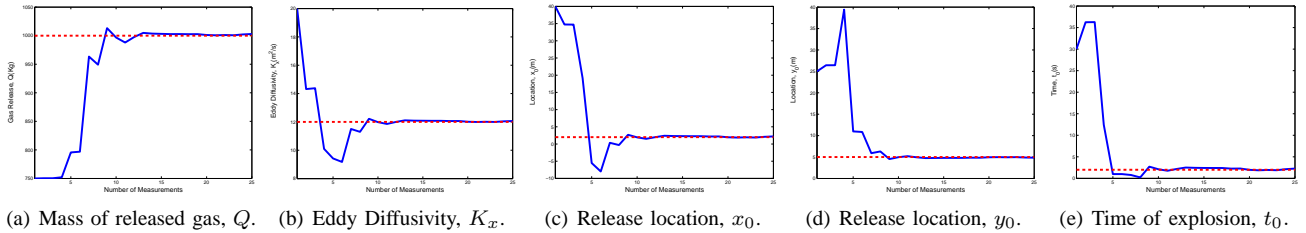


Fig. 8. Convergence of the five estimated parameters using LOT.

A mobile robot moves on flat and obstacle-free terrain with maximum velocity $V_{max} = 1$ m/sec. It starts from the location (20, 30) and collects measurements of the chemical agent concentration every $\Delta T = 4$ sec. The trajectories that the robot follows in each case are shown in Fig. 7. These methods have been tested for three different values of wind velocity. The results show that the LOT and GOT methods generate almost identical robot trajectories. In addition, it should be pointed out that, in most cases, when using the LOT or GOT method, the robot moves in upwind direction, when the wind velocity is higher than its own velocity. On the other hand, the robot moves along the direction of the wind, when its velocity is higher than the wind velocity. However, through a number of simulations, it has been observed that the robot can move in upwind direction even though the velocity of the wind is lower than that of the robot. This means that the robot trajectory does not depend only on the direction and velocity of the wind and thus predefining the trajectory using only these two criteria should be avoided.

A number of 1000 trials have been implemented in order to validate the previous results of the robot trajectories using all aforementioned methods. The starting location of the robot, the speed and direction of the wind, and the maximum robot velocity were uniformly varied. In each trial, it is assumed that the sampling time and starting time of the robot is 4 and 100 sec, respectively. The results show that in 90% of the cases, the LOT approach generates trajectories almost identical to these computed by the GOT.

The trace of covariance matrix for each method is presented in Fig. 4. 50 measurements have been used for each method except for the GOT approach because of its high computational complexity. Observing Fig. 4, the trace of covariance matrix using the LOT method converges faster

and to a lower value compared to the other three approaches (i.e., Anemotaxis, Chemotaxis, Random Walk).

B. Sensitivity Analysis of Initial Estimate Accuracy

In many real-world scenarios, the initial estimate $\hat{\theta}_0$ for certain elements of the unknown parameter vector θ can be close to their actual values. Specifically, for the location x_0 , y_0 and the time t_0 of explosion, a fairly good initial approximation is likely to be available, based on witness of the event. Furthermore, the eddy diffusivity $K_x = K_y$ depends on the type of the chemical gas and the atmospheric conditions, and therefore a good initial guess can be retrieved from precomputed tables. However, in most cases, there is no reliable information about the mass Q of the gas release. For this reason, the initial estimates of Q has been intentionally selected far from its real value. It should be pointed out that an incorrect initial estimate for this or any of the parameters in $\hat{\theta}_0$ may trap the procedure in a local minimum.

We hereafter present a test case where a mobile robot moves on flat and obstacle free area collecting data in order to estimate the parameter vector, θ . The initial information about the values of the estimated parameters is shown in Table II, whereas the constant (known) parameters are listed in Table I. Furthermore, the trajectories of the robot using inaccurate and precise initial estimates for θ are shown in Fig. 5. As evidenced from Fig. 8, the elements of the estimated parameter vector $\hat{\theta}_k$ converge to their real values even though the initial estimate $\hat{\theta}_0$ (i.e., the initial information provided to the robot) is inaccurate. Convergence is achieved when the robot processes the 12th recorded measurement of the gas concentration. Regarding the trajectory, and for the depicted initial position x_1 , y_1 of the robot, the LOT approach dictates that the robot moves along the direction of the wind while approaching the point

of the highest concentration of the chemical agent. This behavior is the same for both an imprecise and an accurate initial estimate for θ . In addition, the robot trajectory is almost the same for both GOT and LOT, although there is a small deviation at the beginning of the procedure. This deviation remains until the robot processes the 5th measurement.

VI. CONCLUSIONS

This paper addresses the problem of estimating the parameters associated with an instantaneous gas release in time critical situations. Using an advection-diffusion model for the propagation of the release, a new approach has been developed that is a combination of a nonlinear least-squares estimation and a locally optimal trajectory generation technique. The main contribution of this work is that the LOT technique, results in a reasonable approximation of the optimal solution in real-time. In addition, LOT and GOT approaches generate almost identical robot trajectories. It should be pointed out that LOT, has linear, in the number of measurements, computational cost and can be implemented in robotic systems with limited processing capabilities. On the other hand, the GOT and generally “brute force” methods have exponential, in the number of measurements, computational complexity and their implementation in a real world scenario require prohibitively high computational resources.

VII. ACKNOWLEDGEMENTS

This work was supported by the University of Minnesota (DTC) and the National Science Foundation (ITR-0324864, MRI-0420836).

TABLE I
CONSTANT PARAMETERS.

Parameter		Units	Values
Mean Wind Velocity	u	m/sec	0.5
Maximum Velocity of the robot	V_{\max}	m/sec	1
Sampling time	ΔT	sec	4
Initial Position of the robot	$x(t_1)$	m	20
Initial Position of the robot	$y(t_1)$	m	40
Initial time	t_1	sec	100
Eddy Diffusivity in Z axis	K_z	m ² /sec	0.2113
Signal to Noise Ratio (SNR)	α^2		$5 \cdot 10^3$

TABLE II
REAL, INITIAL, AND ESTIMATED VALUES OF THE PARAMETERS.

Parameter		Units	θ	$\hat{\theta}_0$	$\hat{\theta}_k$
Gas Release Mass	Q	Kg	1000	750	1001.50
Eddy Diffusivity	K_x	m ² /sec	12	20	12.050
Location of Explosion	x_0	m	2	40	2.150
Location of Explosion	y_0	m	5	25	4.970
Time of Explosion	t_0	sec	2	30	2.120

REFERENCES

[1] E. S. Lee, “Clinical Manifestations of Sarin Nerve Gas Exposure,” *American Medical Association*, vol. 290, no. 5, pp. 659–662, Aug. 2003.

[2] A. Kalelkar, “Investigation of large-magnitude incidents: Bhopal as a case study,” in *Institute of Chemical Engineers, Conference on Preventing Major Chemical Accidents*, Cambridge, MA, May 1998.

[3] D. Zarchitsky, D. F. Spears, D. R. Thayer, and W. M. Spears, “Agent- Based Chemical Plume Tracing using Fluid Dynamics,” in *Proceedings of Formal Approaches to Agent-Based Systems (FAABS III)*, 2004.

[4] D. Zarchitsky, D. F. Spears, W. M. Spears, and D. R. Thayer, “A Fluid Dynamics Approach to Multi-Robot Chemical Plume Tracing,” in *Proceedings of the Third International Joint Conference on Autonomous Agents and Multi Agent Systems*, New York, NY, July 2004.

[5] A. Lilienthal, D. Reinmann, and A. Zell, “Gas Source Tracing with a Mobile Robot Using an Adapted Moth Strategy,” in *Proceedings of Autonomous Mobile Systems*, Stuttgart, Germany, Dec. 2003, pp. 150–160.

[6] A. Dhariwal, G. S. Sukhatme, and A. A. G. Requicha, “Bacterium - inspired Robots for Environmental Monitoring,” in *Proceedings of the IEEE International Conference of Robotics and Automation*, New Orleans, LA, May 2004, pp. 1436–1443.

[7] H. Ishida, K. Suetsugu, T. Nakamoto, and T. Moriizumi, “Study of an Autonomous Mobile Sensing System for Localization of Odor Source Using Gas Sensors and Anemometric Sensors,” *Sensors and Actuators A*, vol. 45, pp. 153–157, 1994.

[8] H. Ishida, Y. Kagawa, T. Nakamoto, and T. Moriizumi, “Odor-source localization in the clean room by an autonomous mobile sensing system,” *Sensors and Actuators B*, vol. 33, pp. 115–121, 1996.

[9] R. Russell, D. Thiel, R. Deveza, and A. Mackay-Sim, “A Robotic System to Locate Hazardous Chemical Leaks,” in *Proceedings of the IEEE International Conference on Robotics and Automation*, Nagoya, Japan, May 1995, pp. 556–561.

[10] A. Hayes, A. Martinoli, and R. Goodman, “Swarm Robotic Odor Localization,” in *Proceedings of the IEEE International Conference on Intelligent Robots and Systems*, Maui, HI, Oct. 2001, pp. 1073–1078.

[11] J. A. Farrell, W. Li, S. Pang, and R. Arrieta, “Chemical Plume Tracing Experimental Results with a Remus A.U.V.” in *Proceedings of the Ocean Marine Technology and Ocean Science Conference*, San Diego, CA, Sep. 2003.

[12] G. Evensen, “The Ensemble Kalman Filter: theoretical formulation and practical implementation,” *Ocean Dynamics*, vol. 53, no. 4, pp. 343–367, November 2003.

[13] G. T. Nofsinger and K. W. Smith, “Plume Source Detection using a Process Query System,” in *Proceedings of the Defense and Security Symposium Conference*. Bellingham, WA: SPIE, Apr. 2004.

[14] H. Versteeg and W. Malalasekera, *Introduction to computational fluid dynamics. The finite volume method*. Longman Scientific and Technical, 1995.

[15] R. M. P. Kathirgamanathan, R. McKibbin, “Source term estimation of pollution from an instantaneous point source,” *Research Letters in the Information and Mathematical Sciences*, vol. 3, no. 1, pp. 59–67, April 2002.

[16] —, “Source release-rate estimation of atmospheric pollution from non-steady point source - part [1]: Source at a known location,” *Research Letters in the Information and Mathematical Sciences*, vol. 5, pp. 71–84, June 2003.

[17] —, “Source release-rate estimation of atmospheric pollution from a non-steady point source - part [2]: Source at an unknown location,” *Research Letters in the Information and Mathematical Sciences*, vol. 5, pp. 85–118, June 2003.

[18] A. Lilienthal and T. Duckett, “Creating Gas Concentration Gridmap with a Mobile Robot,” in *Proceedings of the IEEE International Conference on Intelligent Robots and Systems*, Las Vegas, NV, Oct. 2003, pp. 118–132.

[19] G. Yeh and C. Hug, “Three-Dimensional Air Pollutant modelling in the Lower Atmosphere,” *Boundary-Layer Meteorology*, vol. 9, pp. 381–390, 1975.

[20] D. Luenberger, *Linear and Nonlinear Programming*, 2nd ed. Addison-Wesley, 1984.

[21] V. N. Christopoulos and S. I. Roumeliotis, “Adaptive Sensing for Instantaneous Gas Release Parameter Estimation,” University of Minnesota, Tech. Rep., June 2004, www.cs.umn.edu/~vchristo/Technical.Report.pdf.